Macromolecules

ARTICLE

pubs.acs.org/Macromolecules

Tailored Nanoparticles for Enhancing Polymer Adhesion

Gregory M. Su,[†] Katherine Best,[‡] Thangamani Ranganathan,[‡] Todd Emrick,[‡] and Alfred J. Crosby*[,‡]

[†]Department of Chemical Engineering and [‡]Department of Polymer Science and Engineering, University of Massachusetts Amherst, Amherst, Massachusetts 01003, United States

Supporting Information

ABSTRACT: Nanoparticles are known to affect the physical properties of bulk polymer materials. Here, we report the ability of metal nanoparticles, tailored with chemically matched short polymer ligands, to enhance interfacial properties, specifically the self-adhesion of a polymer melt. Gold nanoparticles functionalized with low-molecular weight (MW ~ 1500 g/mol) polystyrene ligands were introduced to the surface of a polystyrene film (MW ~ 278 kg/mol, PDI = 1.07). A second polystyrene film was brought into contact with the nanoparticle-decorated surface, and subsequently annealed. The resulting interface was characterized with the double cantilever beam (DCB) method to determine the critical strain energy release rate, G_c, of the welded interface as a function of nanoparticle surface coverage. The interfacial strength (G_c) increased with nanoparticle area fraction until a maximum G_c is achieved at an optimal value of nanoparticle coverage. The value of G_c increased by approximately 100% relative to a sample without nanoparticles. This enhancement of interfacial adhesion reveals the potential for utilizing nanoparticles to improve mechanical properties of polymer interfaces.

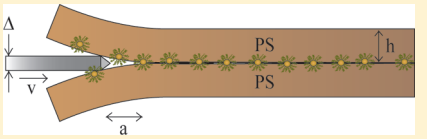

INTRODUCTION

Interfacial properties, such as adhesion, play an important role in the performance of components in many areas including the electronics, automotives, aerospace, and biomedical industries. Accordingly, it is desirable to find ways to enhance the strength of polymer interfaces while maintaining characteristic bulk properties for a given application.

Inorganic nanoparticles (NPs), specifically those tailored with polymer ligands designed to interact synergistically with a surrounding polymer matrix, can greatly influence the mechanical properties of a glassy polymer matrix.[1−5] This influence is strongly dictated by the nature of the matrix−particle interface. Considerable work has focused on NPs that strongly interact with a surrounding matrix to facilitate stress transfer and enhanced stiffness. However, NPs with polymer ligands that weaken interactions with the surrounding matrix have also been shown to positively impact the balance of critical materials properties.[5,6] For example, the addition of weakly interacting NPs to bulk polystyrene alters the high strain mechanical properties and mechanisms of failure. At an optimal volume fraction, NPs significantly increase the failure strain of the otherwise brittle polystyrene (PS), by altering the microstructure of the polystyrene craze, which preempts complete fracture.[1] While increasing ductility significantly, the NPs only modestly decrease the elastic modulus, E, and glass transition temperature, T_g.[7]

Beyond changing bulk properties,[8] it has also been demonstrated that tailored NPs can interact favorably with polymer interfaces. For example, NPs can spontaneously self-assemble, similar to diblock copolymers, at immiscible polymer fluid interfaces. This effect is driven by a reduction of interfacial tension, leading to a decrease in total free energy.[9] Also, it has been demonstrated that for enthalpically neutral NPs in a block copolymer, NPs that are considered large relative to the domain size, remain in the center of the domain, while small NPs migrate to the interface.[10,11] Furthermore, NPs can stabilize interfaces leading to a suppression of polymer film dewetting,[12,13] and fill in cracks in polymer surfaces.[14,15] Although these examples of interfacial mobility combined with the demonstrated impact on bulk properties suggest the potential for using NPs to enhance interfacial strength, to the best of our knowledge there have been limited studies on the quantitative effect of NPs on adhesion. Here, we address the ability of NPs on a polymer surface to affect adhesion by demonstrating a simple concept for controlling the strength of a glassy polymer interface.

Specifically, we show that adhesion, as measured by the critical energy release rate, G_c, for separating an interface, is dictated by the area fraction of the functionalized NPs at the interface. The NPs are tailored with surface ligands that match the chemistry of the two polymer melts, and have a size similar to the radius of gyration, R_g, of the polymer molecules in the melt. Although a wide experimental parameter space exists, our current focus is on the NP area fraction at the welded interface.

EXPERIMENTAL SECTION

Adhesion Characterization via Symmetric Double Cantilever Beam Specimen. The symmetric DCB test is a straightforward method to quantify G_c at a glassy polymer interface. In this process, a crack is propagated at the polymer−polymer interface by driving a razor blade at a constant, slow velocity, v. At steady state, the crack length, a, ahead of the razor blade remains relatively constant, and if the specimen

Received: March 11, 2011
Revised: June 9, 2011
Published: June 16, 2011

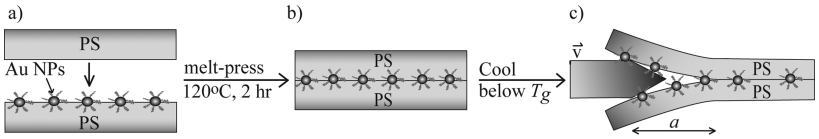

Figure 1. Overall experimental approach. (a) Two PS plaques, one of which contains a layer of Au NPs, are brought together and heated at 120 °C for 2 h under pressure in a melt-press to form (b) a self-adhered PS sample with NPs at the PS−PS interface. After cooling to room temperature, (c) a symmetric DCB specimen test is used to quantify adhesion by driving a razor blade through the interface at a constant velocity, v, while the crack length, a, is monitored.

geometry and elastic moduli of the polymer plaques are known, then G_c can be determined from a.[23]

$$G_c = \frac{3\Delta^2 E h^3}{16 a^4 \alpha^2} \quad (1)$$

where

$$\alpha = \frac{1 + \frac{1.92h}{a} + 1.22\left(\frac{h}{a}\right)^2 + 0.39\left(\frac{h}{a}\right)^3}{\left(1 + \frac{0.64h}{a}\right)} \quad (2)$$

E is elastic modulus of the specimen plaques, h is the thickness of the polymer sample, and Δ is the thickness of the razor blade. Here, the DCB test geometry is exploited to quantify the nanoscale effects of tailored NPs on adhesion via readily measurable, macroscale parameters.

All mechanical tests were performed at room temperature. A single-edge razor blade was inserted at the interface of the adhered PS plaques to initiate a crack, and then driven at a constant velocity of 10 μm/s to propagate the crack. The razor blade was mounted to, and translated by, an automated Newport motorized actuator controlled by LabVIEW software. A camera mounted above the sample collected images of crack propagation every 10 s. Images were analyzed with ImageJ to determine the crack length as a function of time. The elastic modulus, E, of the PS plaques was measured to be 1.40 ± 0.073 GPa by uniaxial tensile testing. A schematic of the general procedure is shown in Figure 1.

Synthesis of Surface-Modified Nanoparticles and Solution Preparation. Gold (Au) NPs were synthesized using previously published procedures[24] with an average diameter of ∼4 nm and functionalized with short PS-SH ligands (MW ∼ 1500 g/mol) (Supporting Information). The PS-SH ligands were prepared from a thiourea-terminated PS precursor, which was synthesized by atom transfer radical polymerization.[25] NPs were dissolved in toluene to produce solutions of varying volume fractions. A 5 wt % solution of high MW PS (MW = 278 kg/mol, PDI = 1.07, Polymer Source) in toluene was prepared for coating the bulk PS plaques with a layer of well-defined polymer chains. Additionally, a 1 wt % solution of low MW PS (MW = 1900 g/mol, Polymer Source) in toluene was used in the fabrication of control samples.

Sample Preparation. The PS samples used for DCB testing consisted of two PS (MW = 350 kg/mol, PDI = 2.0, Aldrich) plaques that were heated under pressure at 150 °C (T_g + 50 °C) in a melt press and formed into plaques measuring ∼50 × 50 × 2.3 mm^3. To minimize effects related to polydispersity, a film of low-polydispersity PS was floated onto the surface of all plaques. The low-polydispersity PS films, measured to be 300 nm thick by a Filmetrics Thin-Film Analyzer F20 interferometer, were produced via flow coating[26] a 5 wt % PS solution in toluene onto a silicon wafer. After drying, the film was floated in water, placed on top of the PS plaques, and annealed at ∼130 °C for 3 h. All flow coating was performed at a constant translational velocity of 7 mm/s and a gap height of 300 μm.

Three interface types were defined with the following subsequent procedures:

Nanoparticle Interface. A solution with a specified volume fraction of PS-functionalized Au NPs in toluene was flow coated on top of the PS plaques.

Low MW Interface. A 1 wt % solution of low MW PS was flow coated on top of the PS plaques.

Solvent Treated Interface. Pure toluene solvent was flow coated on top of the PS plaques.

As an independent control, "neat interfaces", without NPs or subsequent treatment, were also prepared.

Two plaques, one with a surface modified according to one of the three interface treatments listed above, and one nontreated, were brought together and annealed in a melt-press at 120 °C (T_g + 20 °C) for 2 h. The resulting adhered plaques were cooled to room temperature and cut into strips ∼50 × 5 × 4.6 mm^3 with a circular diamond saw and then tested with the DCB method as described above.

RESULTS

It is well-established that the adhesion, or G_c, of glassy amorphous homopolymer interfaces depends on the degree of entanglement among polymer chains, which form effective binding "stitches" at the interface.[16−21] Therefore, G_c increases with the degree of polymerization, N, of the bulk homopolymer until the maximum entanglement density is reached.[20,22] G_c also increases with the square root of contact time as homopolymer interfaces are annealed above the glass transition temperature, T_g.[17] Therefore, maximum adhesion, or fracture toughness approaching that of the bulk, develops at long times at temperatures above T_g. The primary question of interest for this study was to determine if inorganic NPs modified with short PS ligands can enhance the adhesion of a glassy polystyrene interface at short times.

To deposit NPs onto a polymer surface, we used a simple method of flow coating a "wet film" of a NP solution, with height h_{wet} and volume fraction φ. The NPs employed in this system were surface-modified with PS ligands, allowing for uniform dispersion without aggregation on the PS film. PS thin films coated with solutions of NPs of varying φ were imaged with a TEM (JEOL TEM200CX), as depicted in Figure 2. It is evident that PS surface-modified NPs were well dispersed in PS over a range of concentrations. Additionally, these images demonstrate that the area coverage of NPs near the PS interface scales with the volume fraction of NPs in the deposited solution, proving that interfacial NP coverage can be adjusted by simply altering solution concentration. The number of NPs per unit surface area is proportional to the volume fraction of the NP solution in the following manner

$$\frac{\text{no. of NP}}{A} \propto \varphi\left(\frac{h_{wet}}{D_{NP}{}^3}\right) \quad (3)$$

dx.doi.org/10.1021/ma200561g |Macromolecules 2011, 44, 5256–5261

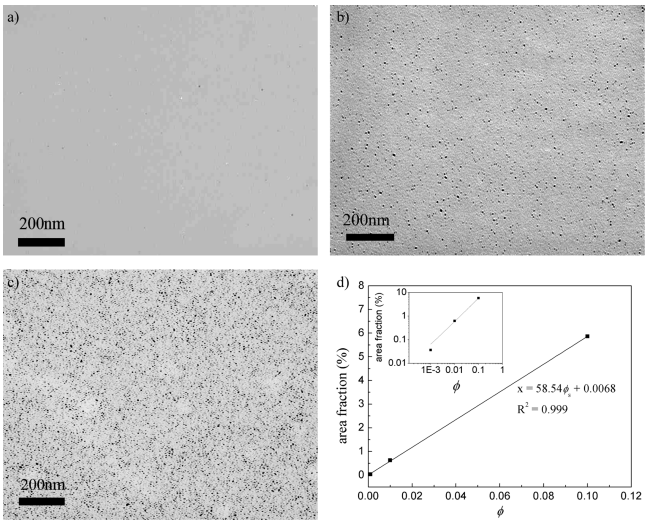

Figure 2. TEM micrographs of PS thin films flow coated over with Au NP solutions of varying NP volume fractions, φ: (a) 0.001%, (b) 0.01%, and (c) 0.1%. (d) Plot of the surface area fraction of the NPs calculated from images a−c as a function of φ. It is evident that NP area coverage scales linearly with solution concentration and NPs are well dispersed in PS. Inset in (d) is a plot same data on log-log axes.

where D_{NP} is the diameter of the NP. Since the factor (h_{wet}/D_{NP}^3) is maintained relatively constant in our experiments by maintaining consistent flow coating parameters, variations in NP area coverage can be achieved by simply altering the φ of the NP solution, as evident in Figure 2.

The strength of the welded interface, G_c, was quantified using the DCB method as described above with eq 1. Accordingly, it was found that interfacial strength increased as a function of NP areal coverage until reaching a maximum value of G_c, nearly twice the neat interfacial strength, at $\varphi \sim 0.07\%$ (Figure 3).

Although Figure 3 demonstrates that the NP areal coverage has a strong influence on interfacial strength, the simplicity of our interface fabrication presents some complexity. To confirm the role of the nanoparticles on controlling G_c, we conducted two sets of control experiments.

Toluene is a good solvent for PS; therefore, it is expected that the toluene will swell the underlying PS and cause disruptions in surface topology when the toluene solution of NPs is flow coated directly onto a PS film. To verify that this swelling does not contribute significantly to the observed adhesion enhancement, an experimental control test of the solvent treated interface was carried out in an identical procedure as described earlier, except a film of toluene only was flow coated onto one of the low-polydispersity PS films. This solvent treated interface was tested in the DCB specimen in the same manner, and the results are included in Figure 4. Solvent treated samples exhibit adhesion similar to that of the neat samples, much lower than the G_c at the optimal value of $\varphi \sim 0.07\%$.

Studies into the effect of the NP capping ligands were undertaken to further ensure that interfacial adhesion enhancement is a result of the combined core-ligand and not ligands alone. The short PS ligands (MW ∼ 1500 g/mol) attached to the NPs may act as plasticizing agents and accordingly alter adhesion. To probe this effect, a test of the low MW interface was performed in which a solution of low MW PS (1900 g/mol, Polymer Source) was flow coated onto one of the low-polydispersity PS films

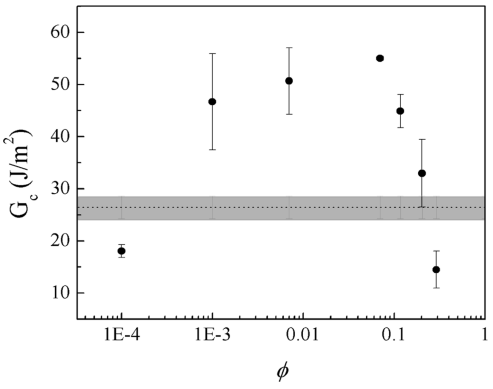

Figure 3. Adhesion of PS−PS interfaces as a function of Au NP solution volume fraction, φ. The greatest increase in adhesion was observed for $\varphi \sim 0.07\%$. The dotted line represents the average G_c for a neat sample with one standard error shaded.

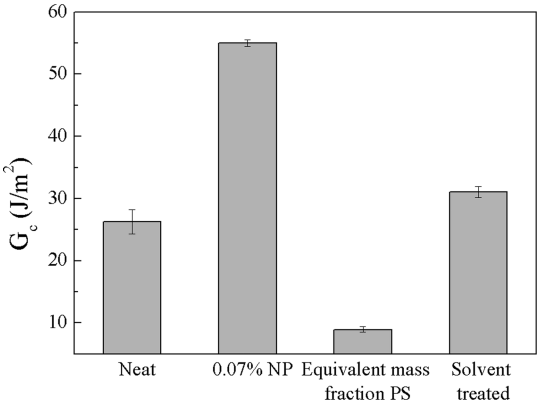

Figure 4. Plot of the adhesion, G_c, of the low molecular weight and solvent treated interfaces compared to the neat interface and the optimal case (φ = 0.07%).

instead of a NP solution. It was calculated that a 1 wt % solution of low MW PS in toluene correlates to the same mass fraction of PS ligands present in the optimal φ = 0.07% NP solution (Supporting Information). It was found that this low MW interface sample resulted in weakened adhesion relative to the neat samples, indicating that the NP ligands are not responsible for the observed enhancement in adhesion. The results are shown in Figure 4.

DISCUSSION

We have shown that a significant enhancement of the interfacial self-adhesion of glassy PS is achieved by deposition of PS-functionalized Au NPs at the PS−PS interface. The simplicity of this approach is appealing, but it would be helpful to identify a primary mechanism for this effect to generalize the approach for other materials systems. Although no proven mechanism currently exists, insight can be gained by considering previous studies concerning the impact of NPs on the mechanical properties of a polymer matrix on a similar system.[7] Accordingly, we have identified three possible mechanisms that could contribute to the demonstrated impact of NPs on adhesion: NPs may (1) alter the mobility of polymer matrix chains, (2) modify the effective local chain end density due to capping ligands, or (3) change the fracture mechanism.

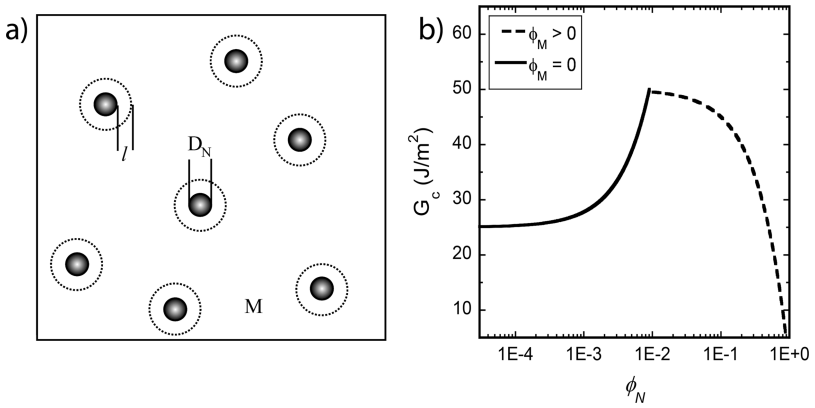

Figure 5. (a) Schematic of a NP composite indicating variables definitions. (b) Calculated G_c as a function of nanoparticle area fraction, where $k = 2$, $l = 10$ nm, as described in the text.

As discussed above, NPs have been shown previously to decrease the glass transition temperature, or increase the mobility of matrix polymer chains, in systems where the NP/polymer interaction is weak.[5,6] In our experiments, this effect could cause polymer chains near NPs and near the bonded interface to migrate at an enhanced rate; thus forming more entanglements along the interface for a given time and temperature of self-adhesion. An increased number of entanglements would lead to enhanced adhesion. Furthermore, as the area fraction of NPs at the interface increases the maximum possible number of polymer entanglements would decrease, thus leading to a decrease in interfacial strength at higher area fractions of NPs. This effect is observed; Indicating that competition between a localized increase in the mobility of neighboring polymer chains and the overall decrease of polymer surface area as a function of increasing NP surface coverage is a plausible mechanism.

However, a straightforward calculation indicates that an increase in mobility leading to an optimization of polymer entanglements is not a likely mechanism. To simplify calculations, an area of the nanoparticle−polymer composite was considered, Figure 5, rather than a volume.

The total area, A_T, consists of the area fraction occupied by the matrix polymer with mobility of bulk PS (φ_M), the area fraction of NPs (φ_N), and an assumed area fraction of enhanced polymer mobility at the NP interface (φ_I), such that

$$\varphi_M + \varphi_I + \varphi_N = 1 \tag{4}$$

The areal concentration of entanglements can be written as

$$\frac{N_E}{A_T} = \frac{1 - \varphi_N - (1-k)\varphi_I}{{R_{g,e}}^2} \tag{5}$$

where k is a constant representing a modified concentration of entanglements within the interface region, N_E is the number of entanglements, and ${R_{g,e}}^2$ is the radius of gyration of PS at its entanglement molecular weight. From geometry,

$$\varphi_I = \varphi_N\left(1 + \frac{l}{D_N}\right)\left(\frac{l}{D_N}\right), \quad \text{for } \varphi_M \geq 0 \tag{6}$$

where l is the width of the interfacial region and D_N is the NP diameter. Substituting eq 6 into eq 5 yields

$$\frac{N_E}{A_T} = \frac{1 + \left[(k-1)\left(1 + \frac{l}{D_N}\right)\left(\frac{l}{D_N}\right) - 1\right]\varphi_N}{{R_{g,e}}^2} \tag{7}$$

This relationship is valid in the regime where the area of the matrix is greater than zero, but at a critical concentration of NPs where the interfacial regions impinge, φ_M is zero. In this regime, $\varphi_I + \varphi_N = 1$ and

$$\frac{N_E}{A_T} = \frac{k(1-\varphi_N)}{{R_{g,e}}^2} \tag{8}$$

To make comparison to our fracture experiments, we assume

$$G_c \sim C\left(\frac{N_E}{A_T}\right) \tag{9}$$

where C is a material constant and plot G_c with respect to NP concentration in Figure 5b. This plot assumes that $k > 1$ (specifically $k = 2$), or entanglements are enhanced at the interface region to account for an increase in G_c. The value of $l \sim 10D_N$ was chosen such that the maximum value for G_c occurs at a NP concentration within the same order of magnitude as that observed in our experiments. This value implies that the interfacial zone around the NP, where chain mobility is increased, is approximately 50 nm, which is significantly larger than other relevant length scales in our materials suggesting that this mechanism is unlikely.

In addition to mechanisms related to the excluded volume of a rigid, weakly interacting NP, short PS ligands present on the surface of the NPs may also play a role in increasing the rate of entanglement formation by increasing the PS chain end density at the interface.[28] This effect is well-known as described by the bulk plasticization of PS with short PS chains.[27] To test this mechanism, we conducted a control experiment with short PS chains dispersed at the interface in the absence of NPs. The results of the control experiment (Figure 4) verified that these short chains at the interface do not enhance adhesion, but instead decrease it. Therefore, the presence of a rigid nanoparticle core is important for developing an enhanced level of adhesion at a given temperature and time.

Beyond altering the mobility of neighboring chains, the presence of weakly interacting NPs has been demonstrated to alter the fracture mechanism of amorphous PS. Lee et al. demonstrated that CdSe NPs surface-modified with short PS ligands can increase the failure strain of typically brittle PS thin films, with a maximum increase of nearly 100% occurring at an optimal NP volume fraction of 0.7%. Polystyrene, as with many glassy polymers, generally fails through the formation of crazes, which are interpenetrating microvoids and fibrils that often

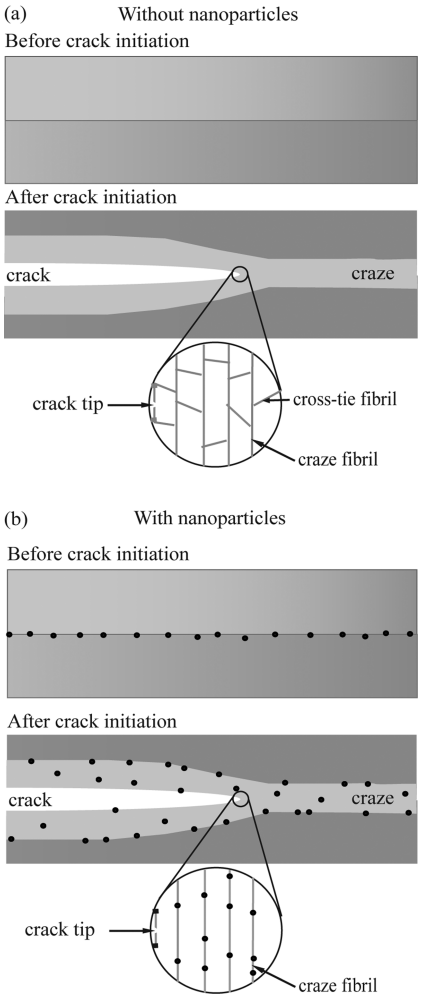

Figure 6. Schematic of potential mechanism of the effect of nanoparticles on crack growth at a polymer interface. (a) Without nanoparticles stress around the crack leads to formation of characteristic crazes and subsequent fibrils and cross-tie fibrils. (b) The presence of nanoparticles disrupts the formation of cross-tie fibrils leading to an increase in G_c. The decrease in cross-tie fibrils is exaggerated for schematic purposes.

precede fracture. In NP−PS composites, it has been found that NPs lead to an increase in G_c by interfering with the formation of craze cross-tie fibrils, as shown in Figure 6, which connect main fibrils providing lateral load transfer to facilitate cracking. Disrupting cross-tie fibrils prevents lateral load transfer therefore, effectively "blunting" a propagating crack and increasing G_c.[1] It is possible that a mechanism similar to the disruption of craze cross-tie fibrils, which was previously observed directly with TEM in thin films, is responsible for the observed enhancement of PS interfacial self-adhesion in the current experiments. This is supported by the fact that the PS-covered Au NPs in our system disperse well in PS, and the peak in the plot of G_c vs φ is qualitatively similar to the peak in strain of failure vs NP volume fraction observed in a previous study on PS-NP composite films.[1] Also, X-ray photoelectron spectroscopy (XPS) data (Supporting Information) of the two fracture surfaces of a PS−PS interface following a DCB test verify that Au is present on both sides, even though NPs are initially deposited on only one surface. This supports the ability of NPs to penetrate both sides of the matrix at the interface and impact craze formation. A schematic of the potential effect of NPs on the crazing mechanism at the interface is depicted in Figure 6.

In addition to the increase in adhesion, Figure 3 reveals a reduction in G_c at low and high φ. Again, this observation is consistent with the craze/fracture observations of Lee et al.[1] At very low φ, there are too few NPs to significantly disrupt cross-tie fibril formation; whereas, at very large φ, the dense layer of NPs hinders interpenetration and entanglement of polymer chains at the interface. Therefore, a decrease in the as-prepared polymer entanglement density is hypothesized at high values of φ, consistent with the findings and theory presented previously.[1] Direct visualization of this proposed mechanism is challenging due the disruption of craze surfaces in postfracture sample preparation, but experiments are currently being conducted to provide future, quantitative insight.

CONCLUSION

We have demonstrated that PS-functionalized Au NPs increase the self-adhesion of a glassy PS−PS interface. This control of interfacial strength is achieved by a straightforward method of NP deposition and characterized with the classical, symmetric double cantilever beam fracture test geometry. At an optimal NP solution volume fraction of 0.07%, the critical energy release rate, G_c, was found to increase by approximately 100% relative to a neat sample. Control experiments reveal that solvent swelling and short PS chains alone will not lead to enhanced adhesion. The mechanical advantages that NPs exhibit along with their unique electronic and optical properties demonstrate the potential to produce advanced nanomaterials with numerous enhanced functionalities.

ASSOCIATED CONTENT

Supporting Information. Derivation of solution concentration for the low molecular weight interface, XPS data verifying that gold is present on both sides of a fractured surface, and detailed description of nanoparticle functionalization. This material is available free of charge via the Internet at http://pubs.acs.org.

AUTHOR INFORMATION

Corresponding Author

*E-mail: crosby@mail.pse.umass.edu. Telephone: (413) 577-1313. Fax: (413) 542 0082.

ACKNOWLEDGMENT

This work was supported by the Army Research Office (ARO W911NF-08-1-0274) and NSF PIRE (NSF 0730243). We also thank Louis Raboin and Jack Hirsch for technical help with operating the TEM and XPS instruments.

REFERENCES

(1) Lee, J.-Y.; Zhang, Q.; Wang, J.-Y.; Emrick, T.; Crosby, A. J. *Macromolecules* **2007**, *40*, 6406–6412.
(2) Vollenberg, P. H. T.; Heikens, D. *Polymer* **1989**, *30*, 1656–1662.
(3) Ahmed, S.; Jones, F. R. *J. Mater. Sci.* **1990**, *25*, 4933–4942.
(4) Ji, L.; Jing, J. K.; Jiang, W.; Jiang, B. Z. *Polym. Engr. Sci.* **2002**, *49*, 983–993.
(5) Bansal, A.; Yang, H.; Li, C.; Cho, K.; Benicewicz, B. C.; Kumar, S. K.; Schadler, L. S. *Nature Mat.* **2005**, *4*, 693–698.
(6) Green, P. F.; Oh, H. *Nat. Mat.* **2009**, *8*, 139–143.

(7) Lee, J.-Y.; Su, K. E.; Chan, E. P.; Zhang, Q.; Emrick, T.; Crosby, A. J. *Macromolecules* **2007**, *40*, 7755–7757.
(8) Hamming, L. M.; Qiao, R.; Messersmith, P. B.; Brinson, L. C. *Compos. Sci. Technol.* **2009**, *68*, 1880–1886.
(9) Lin, Y.; Skaff, H.; Emrick, T.; Dinsmore, A. D.; Russell, T. P. *Science* **2003**, *299*, 226–229.
(10) Bockstaller, M. R.; Lapetnikov, Y.; Margel, S.; Thomas, E. L. *J. Am. Chem. Soc.* **2003**, *125*, 5276–5277.
(11) Lin, Y.; Boker, A.; He, J.; Sill, K.; Xiang, H.; Abetz, C.; Li, X.; Wang, J.; Emrick, T.; Long, S.; Wang, Q.; Balazs, A.; Russell, T. P. *Nature* **2005**, *434*, 55–59.
(12) Barnes, K. A.; Karim, A.; Douglas, J. F.; Nakatani, H. G.; Amis, E. J. *Macromolecules* **2000**, *33*, 4177–4185.
(13) McConnell, M. D.; Bassani, A. W.; Yang, S.; Composto, R. J. *Langmuir* **2009**, *25* (18), 11014–20.
(14) Gupta, S.; Zhang, Q.; Emrick, T.; Balazs, A. C.; Russell, T. P. *Nat. Mater.* **2006**, *5*, 229–233.
(15) Tyagi, S.; Lee, J. Y.; Buxton, G. A.; Balazs, A. C. *Macromolecules* **2004**, *37*, 9160–9168.
(16) Creton, C.; Kramer, E. J.; Brown, H. R.; Hui, C.-Y. *Adv. Polym. Sci.* **2001**, *156*, 53–136.
(17) Jud, K.; Kausch, H. H.; Williams, J. G. *J. Mater. Sci.* **1981**, *16*, 204–21.
(18) Schnell, R.; Stamm, M.; Creton, C. *Macromolecules* **1999**, *32*, 3420–3425.
(19) Wool, R. P.; Yuan, B. L.; McGarel, O. J. *Polym. Eng. Sci.* **1989**, *29*, 1340.
(20) Brown, H. R. *Annu. Rev. Mater. Sci.* **1991**, *21*, 463.
(21) Schnell, R.; Stamm, M.; Creton, C. *Macromolecules* **1998**, *31*, 2284–2292.
(22) Cole, P. J.; Cook, R. F.; Macosko, C. W. *Macromolecules* **2003**, *36*, 2808–2815.
(23) Kanninen, M. F. *Int. J. Fract.* **1973**, *9*, 83–92.
(24) Brust, M.; Walker, M.; Bethell, D.; Schiffrin, D. J.; Whyman, R. *Chem. Commun.* **1994**, 801–802.
(25) Garamszegi, L.; Conzel, C.; Carrot, G.; Nguyen, T. Q.; Hilborn *J. React. Funct. Polym.* **2003**, *55*, 179–183.
(26) Stafford, C. M.; Roskov, K. E.; Epps, T. H.; Fasolka, M. J. *Rev. Sci. Instrum.* **2006**, *77*, 023908.
(27) Fox, T. G.; Flory, P. L. *J. Appl. Phys.* **1950**, *21*, 581–591.
(28) Guerin, G.; Mauger, F.; Prud'homme, R. *Polymer* **2003**, *44*, 7477–7484.